Influence of Sintering Temperature on Hardness and Wear Properties of TiN Nano Reinforced SAF 2205

S R Oke[1,2], O O Ige[1,3], O E Falodun[1], B A Obadele[1], M R. Mphalele[1] and P A Olubambi[1]

[1] Centre for Nanoengineering and Tribocorrosion, School of Mining, Metallurgy and Chemical Engineering, University of Johannesburg, Doornfontein Campus, Johannesburg, South Africa
[2] Department of Metallurgical and Materials Engineering, Federal University of Technology Akure, Ondo State, PMB 704, Nigeria
[3] Department of Materials Science & Engineering, Obafemi Awolowo University Ile-Ife, Osun State, Nigeria

Abstract. Conventional duplex stainless steel degrade in wear and mechanical properties at high temperature. Attempts have been made by researchers to solve this problems leading to the dispersion of second phase particles into duplex matrix. Powder metallurgy methods have been used to fabricate dispersion strengthened steels with a challenge of obtaining fully dense composite and grain growth. This could be resolved by appropriate selection of sintering parameters especially temperature. In this research, spark plasma sintering was utilized to fabricate nanostructured duplex stainless steel grade SAF 2205 with 5 wt.% nano TiN addition at different temperatures ranging from 1000 °C to 1200 °C. The effect of sintering temperature on the microstructure, density, hardness and wear of the samples was investigated. The results showed that the densities and grain sizes of the sintered nanocomposites increased with increasing the sintering temperature. The microstructures reveal ferrite and austenite grains with fine precipitates within the ferrite grains. The study of the hardness and wear behaviors, of the samples indicated that the optimum properties were obtained for the sintering temperature of 1150 °C.

1. Introduction

Duplex stainless steels are widely used in aerospace, chemical, power generation and biomedical and nuclear industries because of high corrosion resistance, good mechanical strength and ductility, abrasion resistance, erosion resistance and a very good weldability [1-3]. However, these alloys may suffer considerable loss in wear and mechanical strength at elevated temperatures. One promising approach to improve the elevated temperature properties as well as wear and oxidation properties of stainless steels is by reinforcing it with second phase particles [4].

One of the processing methods that can be explored to fabricate dispersion strengthened stainless steels is powder metallurgy (PM) [5]. Hot extrusion (HE), hot isostatic pressing (HIP) and mechanically alloying (MA) are the most frequently used PM processes for the fabrication of dispersion strengthened composites [6-7]. Relatively, spark plasma sintering (SPS) have been reported to be a better technique due to its low energy consumption and very short sintering time. SPS utilizes a pulsed direct electrical current to perform high speed consolidation of powders. Rapid high heating and cooling rates which

characterizes SPS process allow maintaining and improvement of the inherent properties of powders in their fully dense products [8-10]. SPS has been used to fabricate nanostructured composites, thermoelectric materials, ferroelectric materials, magnetic materials and nanograined materials [11].
Sintering temperature is an important process parameter in the consolidation of powders during SPS. Its appropriate selection could be used to control density, grain/crystallite size and porosity of PM parts which may improve mechanical properties [12]. Javanbakht et al., [13] investigated the effect of sintering temperature on structure and mechanical properties of AISI 316L stainless steel. The authors reported that residual porosity reduced with increasing sintering temperature while crystallite/grain sizes were enhanced. The optimum mechanical properties were obtained for the sintering temperature of 1150 °C. In a related study by Li et al. [14], with the increasing of sintering temperature from 950 °C to 1025 °C, the density and average grain sizes of 14Cr-ODS ferritic steels increased from 290 nm to 2420 nm. Sorour et al. [15] investigated the microstructure and tribology of Fe-Cr-B alloy sintered by SPS. They sinter at 1150 °C at a heating rate of 225 °C/min, holding time of 10 min and were able to achieve a hardness value of 991 HV with this alloy.
However, the effects of sintering temperature on nanostructured stainless steels have received attention in recent time. In this study, duplex stainless steels grade SAF 2205 and nano TiN was consolidated via SPS. This report documents a study of the effects of spark plasma sintering temperature on the micro-structure, hardness and wear of TiN nano structured SAF 2205 steel.

2. Experimental procedure

DSS 2205 (particle size about 22μm, supplied by Sandvik Osprey Ltd, UK) and TiN (particle size of 20nm, 97% purity, supplied by Nanostructured & Amorphous Materials, Inc.USA) powders were utilized as the starting materials for this research. The powders were mixed in a dry environment using the Turbula Shaker Mixer T2F at a mixing speed of 72rpm for 8h to ensure homogeneous mixing of powders.
The appropriate amount of mixed powders required to produce 20mm diameter and 5mm thick DSS-TiN nano structured composites were poured into a graphite die and then sintered using an automated spark plasma sintering machine (model HHPD-25, FCT GmbH Germany).
The phases present in the sintered specimen were characterized by X-ray diffraction (XRD) using a PANalytical Empyrean model with Cu Kα radiation and analyzed using Highscore plus software. The samples were etched using carpenters reagent for 20s and the microstructure was analyzed using a scanning electron microscope (FESEM, JSM-7600F, JEOL, Japan) incorporated with an EDX detector (Oxford X-Max) with INCA X-Stream2 pulse analyzer software, and Back Scattered Electron (BSE) detectors.
The Vickers microhardness (Hv) at room temperature was measured by a microhardness tester (Future-tech) at a load (P) 100 gf (1.0 N) and a dwell time of 10 s. Three repeat tests were carried out on the samples to ensure reliability of the data generated. The wear tests were conducted on the universal micro-tribotester (UMT-2, Center for Tribology, Inc.). The samples were fixed onto the precision linear stage. A reciprocating motion based on a crank-slider mechanism was exerted on the fixed samples by a ball under dry condition. The frictional force was measured by the load sensor integrated to the side of the ball holder of the tribotester. A load (P) of 5 N was selected; meanwhile, the sliding length (Ls) and the time of linear reciprocating sliding were fixed to 2 mm and 1000s, respectively.

3. Results and discussion

Figure 1a shows that the nano particles of the TiN were evenly distributed in the 2205 matrix. The XRD result (Figure 1b) of the mixed powders shows that only peaks corresponding to TiN and phases containing iron, chromium, and nickel which are the main constituent of DSS 2205 phases are detected in the patterns. The XRD result of the sintered composites with sintering temperature is presented in figure 2. It is observed from the XRD result that there phase change, and a new phase of iron nitride with chemical formula $FeN_{0.068}$ was formed. There was slight change in relative intensity of peaks which is obviously due to the difference in sintering parameters of temperature.

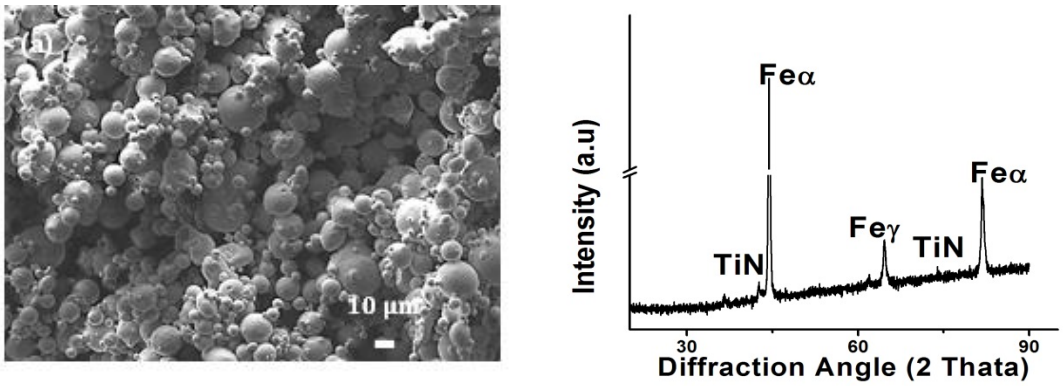

Figure 1. SEM (a) and XRD (b) results of the mixed 2205 duplex stainless steel and TiN powders.

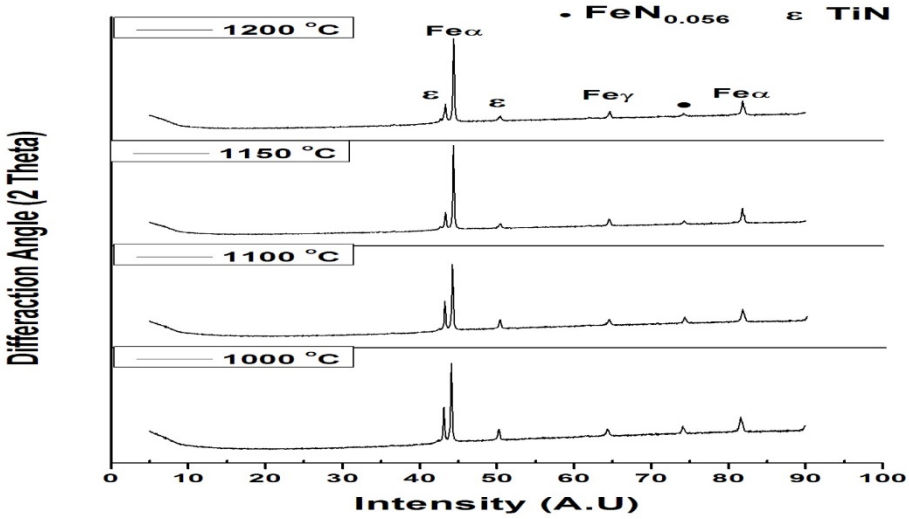

Figure 2. XRD result of sintered DSS 2205-5TiN composite at different temperatures.

The effect of sintering temperatures on the microstructure of the TiN nanostructure SAF 2205 composites is shown in Figure 3. The microstructure consists of austenite and ferrites. The reinforcing TiN phase was uniformly distributed in the duplex matrix. The grains were also observed to grow with increasing sintering temperature. At 1150 ^{o}C (Figure 3c), fine nitride precipitates were detected within the grains and grain boundaries with a higher packing density and an increase in the number of necks which indicates improved sintering. The presence of these precipitates accumulated within the grain and grain boundaries could significantly retard the grain boundary mobility and dislocation movement [5].

Figure 4 presents the density and micro-hardness results with increase in sintering temperature. The figure shows that the density and micro-hardness increased with sintering temperature up to 1150°C. The increase in densification could be attributed to improved powder contact and decrease in porosity level obtained at 1150^{o}C. A reduction in density and hardness was however noted with an increase in sintering temperature to 1200 ^{o}C. The decrease in densification and hardness at 1200^{o}C may be as a result of localized melting of powders. Toor et al., [16] optimized process parameters for Fe-18Cr-2Si, the reported a decrease in density and hardness at sintering temperature 1200 ^{o}C. The authors suggested that partial melting of stainless steel powders could occur at 1200 ^{o}C.

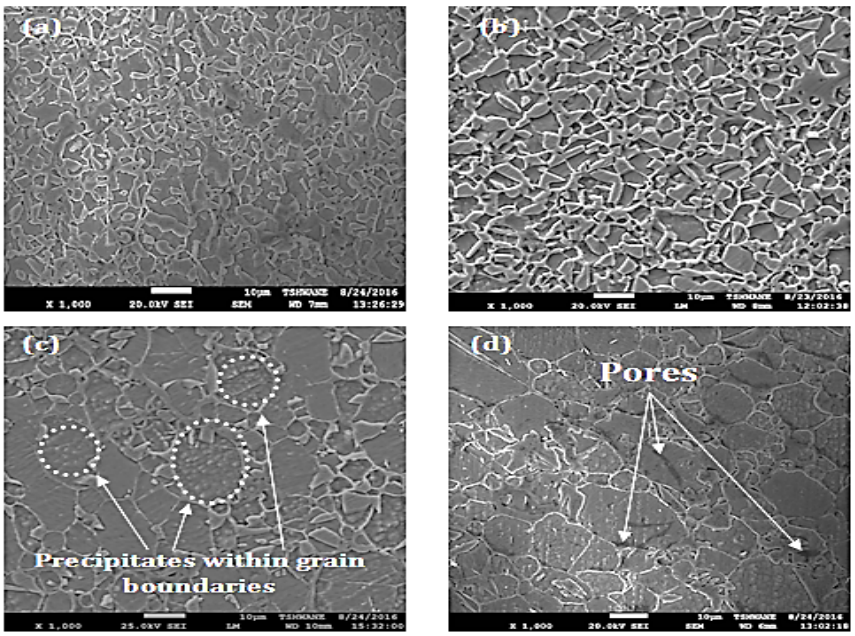

Figure 3. Microstructures of composites with 5 % TiN sintered at (a) 1000 (b) 1100 (c) 1150 and (d) 1200 ^{o}C.

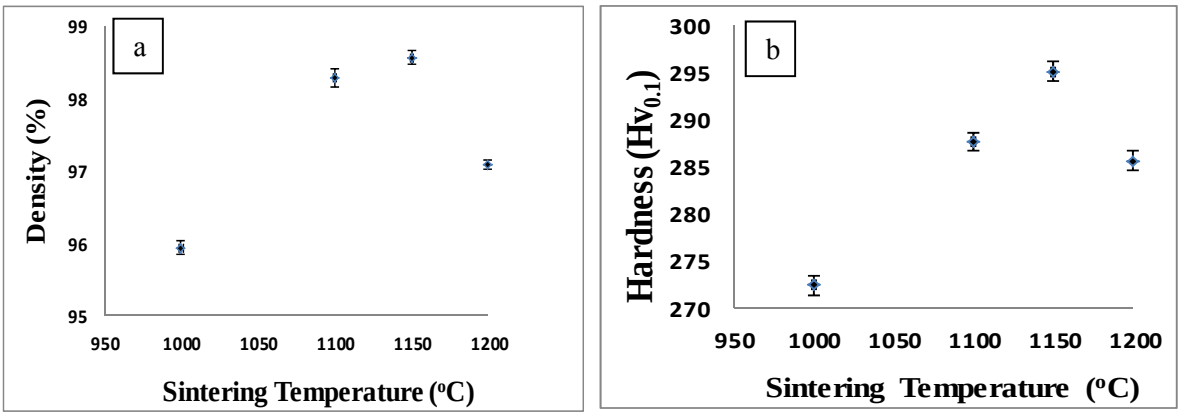

Figure 4. Effect of sintering temperature variation on the (a) densification and (b) hardness of SAF 2205-5TiN.

Figure 5 presents the influence of sintering temperature on coefficients of friction and wear depths of the TiN reinforced SAF 2205 composites over a period of 1000 s. Related frictional behaviors were noticed irrespective of temperature except for the grade sintered at 1000 ^{o}C which shows a high degree of instability. The coefficients of friction (Figure 5a) slightly decreased with increased sintering temperature. However, the coefficients of friction of the grades sintered at 1100 ^{o}C and 1150 ^{o}C were much lower than those of other frictional pairs and were maintained almost constant throughout the testing time. Upon increasing the sintering temperature (1200 ^{o}C), the mean coefficients of friction slightly increased from 0.02 to 0.03. Wear depths as shown in figure 5b linearly increased with increasing time. The composite grade sintered at 1150 ^{o}C exhibited the highest wear resistance. The low coefficient of friction observed for the composite sintered at 1150 ^{o}C could be as a result of its high hardness and densification reported in figure 4.

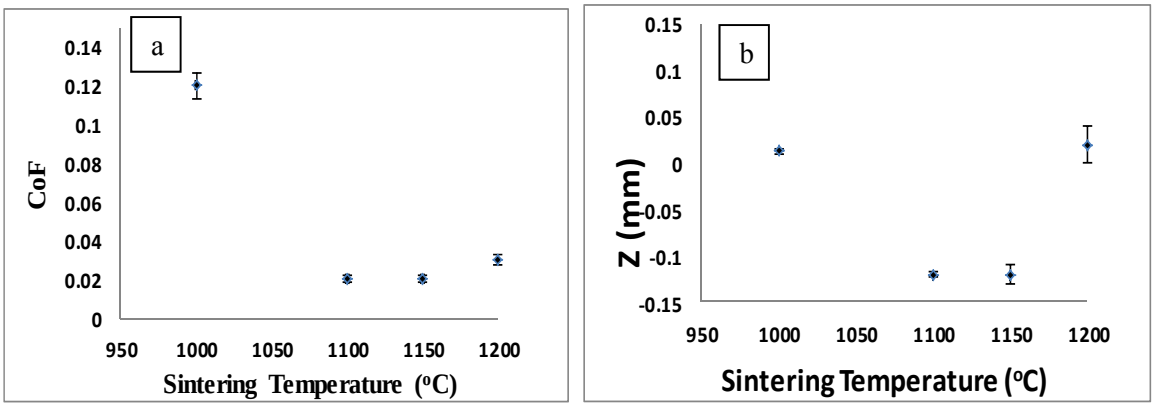

Figure 5. Variation of (a) COF and (b) wear depths of spark plasma sintered SAF 2205-5%TiN powders under different sintering temperature.

The worm surface as observed under the SEM for the grade sintered at 1150 °C is presented in Fig. 6. A series of parallel smooth grooves (Figure 6a) extending longitudinally toward the sliding direction is observed while the material is displaced to the edges, forming a topography that can be described as extruded ridges [17]. The smooth parallel grove observed is obviously due to plastic flow and daubed at the wear track by the sliding friction, which is in agreement with other studies [18].

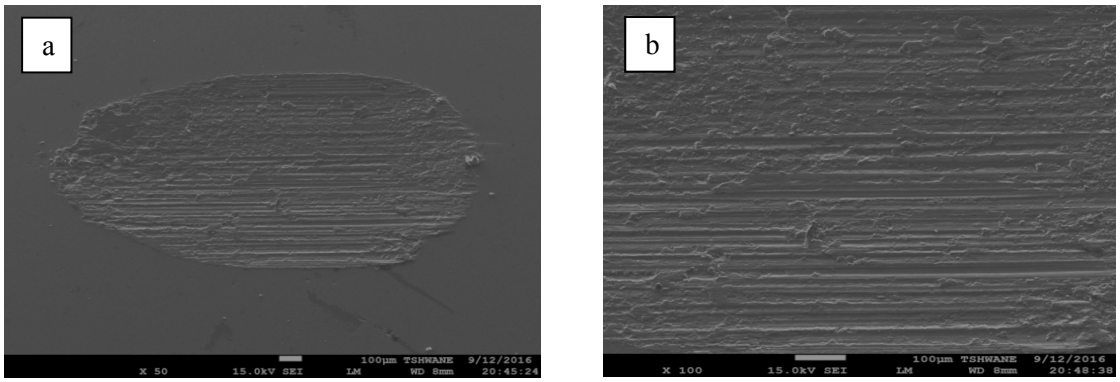

Figure 6. SEM images of the worn surface of the SAF 2205-5TiN composites at 1150 °C.

4. Conclusion

DSS 2205-5%TiN composite had been synthesized by SPS. SPS process parameters were optimized for the composites in terms of their effect on density, hardness and Wear. The results can be concluded as follows;

1. The density and hardness increased with increase in sintering temperature and holding time with maximum densification and hardness achieved at 1150°C
2. The grains were noticed to increase with increasing sintering temperature with fine nitride precipitates within the ferrite grains.
3. For wear, grade sintered at 1150 °C has the highest wear resistance compared to other nano-composite grades.

Acknowledgement

The authors would like to extend appreciation to National Research Foundation (NRF) of South Africa and the Global Excellence and Stature of the University of Johannesburg, South Africa for their financial support.

5. References

[1] T. Karahan, H. E Emre, M Tümer, R. Kaçar, "Strengthening of AISI 2205 duplex stainless steel by strain ageing'', Mater. Des. Vol. 55, pp. 250–256, 2014.

[2] L.A. Dobrzanski, Z. Brytan, M. Actis Grande, M. Rosso, "Properties of duplex stainless steels made by powder metallurgy'', Arch. Mater. Sci. Eng. Vol. 28, pp. 217–223, 2007.

[3] G. Chail, P. Kangas, "Super and hyper duplex stainless steels: structures, properties and applications'', Procedia Structural Integrity, vol. 2, pp. 1755-1762, 2016.

[4] A .Fedrizzi, M. Pellizzari, M. Zadra, E. Marin, "Microstructural study and densification analysis of hot work tool steel matrix composites reinforced with TiB_2 particles'', Mater. Charact. Vol. 86, pp. 69– 79, 2013.

[5] M. Javanbakht, M. Hadianfard, E. Salahinejad, "Microstructure and mechanical properties of a new group of nanocrystalline medical-grade stainless steels prepared by powder metallurgy'', J. Alloys Compd. Vol. 624, pp. 17–21, 2015.

[6] S.R. Oke, O.O. Ige, O.E. Falodun, B.A. Obadele, M.B. Shongwe, P.A. Olubambi. "Optimization of process parameters for spark plasma sintering of nano structured SAF 2205 composite'', J. of Materials Research and Technol, http://dx.doi.org/10.1016/j.jmrt.2017.03.004, 2017

[7] S. Cheng, E. Ma, Y. Wang, L. Kecskes, K. Youssef, C. Koch, "Tensile properties of in situ consolidated nanocrystalline Cu'', Acta Mater. Vol. 53 1521–1533, 2005.

[8] Z..H. Zhang, Z.F. Liu, J.F. Lu, X.B. Shen, F.C. Wang, Y.D. Wang, "The sintering mechanism in spark plasma sintering – Proof of the occurrence of spark discharge'' Scripta Materialia, vol. 81, pp. 56–59, 2014.

[9] S. Diouf, A. Molinari, "Densification mechanisms in spark plasma sintering: Effect of particle size and pressure'', Powder Technology, vol. 221, pp. 220 –227, 2012.

[10] R. Marder, R. Chaim, G. Chevallier, C. Estournes, "Densification and polymorphic transition of multiphase Y2O3 nanoparticles during spark plasma sintering'', Materials Science and Engineering A, vol. 528, pp. 7200-7206, 2011.

[11] I. Sulima, P. Putyra, P. Hyjek, T. Tokarski, "Effect of SPS parameters on densification and properties of steel matrix Composites'', Advanced Powder Technology, vol. 26, pp. 1152–1161, 2015.

[12] G. Ji, F. Bernard, S. Launois, T. Grosdidier, Processing conditions, microstructure and mechanical properties of hetero-nanostructured ODS FeAl alloys pro-duced by spark plasma sintering, Mater. Sci. Eng. A vol. 559, pp. 566 – 573, 2013.

[13] M. Javanbakht, E.Salahinejad, M.J. Hadianfard, "The effect of sintering temperature on the structure and mechanical properties of medical-grade powder metallurgy stainless steels'' Powder Technology, vol. 289, pp. 37–43, 2016.

[14] Z. Li, Z. Lu, R. Xie, C. Lu, C. Liu, "Effect of spark plasma sintering temperature on microstructure and mechanical properties of 14Cr-ODS ferritic steels'', Materials Science & Engineering A, vol. 660, pp. 52– 60, 2016.

[15] A.A. Sorour, H.W. Strauss, R.R. Chromik, M. Brochu, Microstructure and tribology of spark plasma sintered Fe–Cr –B metamorphic alloy powder, Tribol. Lett. Vol. 44, pp.269 –278, 2011.

[16] I. Toor, J. Ahmed, M.A. Hussein, N. Al-Aqeeli, "Optimization of process parameters for spark plasma sintering of nano-structured ferritic Fe-18Cr-2Si alloy'', Powder Technology, vol. 299, pp. 62–70, 2016.

[17] A. Jourani, S. Bouvier S, "Friction and Wear Mechanisms of 316L Stainless Steel in Dry Sliding Contact: Effect of Abrasive Particle Size", Tribology Transactions, vol. 58, no. 1, pp. 131-139, 2015.

[18] P. Tian, N.W. Khun, S.B. Tor, E. Liu, Y. Tian, "Tribological behavior of Zr-based bulk metallic glass sliding against polymer, ceramic, and metal materials'', Intermetallics, vol. 61, pp. 1-8, 2015.